

Cavitation erosion behavior of nickel-aluminum bronze weldment^①

LI Xiao-ya(李 Xia 亚)^{1, 2, 3}, YAN Yong-gui(闫永贵)², XU Zhen-ming(许振明)¹, LI Jian-guo(李建国)¹

(1. State Key Laboratory of Metal Matrix Composites, Shanghai Jiaotong University, Shanghai 200030, China;

2. State Key Laboratory for Marine Corrosion and Protection, Qingdao Branch,

Luoyang Ship Materials Research Institute, Qingdao 266071, China;

3. College of Materials Science and Engineering,

Hebei University of Science and Technology, Shijiazhuang 050054, China)

Abstract: Cavitation erosion behavior of nickel-aluminum bronze(NAB) weldment in 3.5% NaCl aqueous solution was studied by magnetostrictive vibratory device for cavitation erosion. The results show that cavitation erosion resistance of the weld zone(WZ) of the weldment is superior to that of the base metal. SEM observation of eroded specimens reveals that the phases undergoing selective attack by the stress of cavitation erosion at the early stage of cavitation erosion are: martensite in the WZ, α phase in the heat-affected zone(HAZ) and eutectoidal phase in the base metal; the microcracks causing cavitation damage initiate at the phase boundaries.

Key words: NAB; weldment; tungsten inert gas welding(TIG); cavitation erosion

CLC number: TG 172.9

Document code: A

1 INTRODUCTION

Cavitation refers to the nucleation and growth of cavities or bubbles in fast-flowing or vibrating liquid when the local pressure in the liquid drops below a certain level. These bubbles will implode or collapse when they are transported to a high pressure region. The collapse of bubbles is accompanied by the emission of shock waves and micro-jets, which will exert stress pulses on a solid surface in the vicinity. Repetitions of such pressure pulses on solid surfaces will eventually result in fatigue failure and mass loss, and such a mode of damage is known as cavitation erosion^[1]. Cavitation damage usually occurs on propellers, hydraulic turbine blades, vanes, ultrasonic devices and pipelines, etc^[2].

Aluminum bronzes possess high strength, good ductility and excellent corrosion resistance and, hence, are being used to cast propellers, impellers, valves and gearblanks, etc. Welding is a common technology for joining or repairing components. Many researchers did work on aluminum bronzes welding and their post-welding properties. Clews^[3,4] reported metallurgical aspect of aluminum bronze welding problems; Foster et al^[5], composition and microstructure of weldable as-cast studied the NAB; Sahoo et al^[6,7], reported the weldability of NAB. Zanis et al^[8,9] and Lorimer et al^[10] studied corrosion behavior of NAB weldments. However, reports on cavitation erosion of aluminum bronze weldment are rare.

NAB is one of the most commonly-used ship propeller materials. A propeller badly cavitation erosion attacked must be repaired by welding because the efficiency of the propeller falls heavily under this condition. It is very important for us to understand the cavitation erosion resistance and cavitation erosion behavior of the weldment, which can help us to predict the life of the repaired propeller. In this paper, an investigation on the cavitation erosion behavior of NAB weldment was carried out.

2 EXPERIMENTAL

2.1 Specimen preparation

The specimen material was an as-cast ZCCu3 (equivalent to BS NAB, ASTM 148B C95800) plate whose dimensions were 500 mm long, 200 mm wide and 20 mm thick. The casting process of the plate was similar to that of the ZCCu3 propeller. The nominal composition of ZCCu3 was 7% - 11% Al, 2% - 6% Fe, 2% - 6% Ni, 0.5% - 4% Mn and Cu, the balance(mass fraction). The actual composition by wet chemical analysis was 8.56% Al, 4.84% Fe, 4.49% Ni, 1.40% Mn and 79.53% Cu.

A U-groove of 500 mm long, 15 mm wide and 5 mm deep was machined in the middle of the plate. And then the groove was filled with filler material the same as the parent metal with TIG. The welding current was 350 A and voltage, 17 V. The shielding gas was Argon. The weldment was ground smooth after

① **Foundation item:** Project((11H1004) supported by the National Defence Foundation of China

Received date: 2002 - 11 - 28; **Accepted date:** 2003 - 03 - 08

Correspondence: YAN Yong-gui, PhD; Tel: + 86-532-5843198; E-mail: yyg98@vip.sina.com

welding.

Bars of 14 mm in diameter and 20 mm in length were cut from the WZ, the base metal and the area containing WZ, HAZ and base metal, respectively. The round bars were machined to flat-ended studs (12.7 mm in diameter) with a threaded length for attachment to the vibration horn in the cavitation test. The specimens were polished to a constant surface roughness with 1 μm diamond paste, and then cleaned and degreased before the cavitation test.

2.2 Vibratory cavitation erosion test

The test rig was a magnetostrictive vibratory device. The test specimen was screwed to the free end of an amplifying magnetostrictive vibratory horn (open beaker method ASTM G32^[11]). The horn frequency was 20 kHz. The double amplitude (peak to peak) was 60 μm . The test liquid was 3.5% NaCl aqueous solution kept at 25 ± 2 °C.

Before and after each subsequent cavitation erosion test, all specimens were cleaned, dried, and weighed by Sartorius BS210S balance with sensitivity to 0.1 mg.

2.3 Specimen observation

Metallographic specimens of the NAB weldment containing the WZ, HAZ and base metal were cut, ground and polished, and then etched with ferrite chloride (FeCl_3) aqueous solution. The microstructure of the specimens was analyzed by optical microscopy (Olympus PME3). The morphology of the specimens exposed to cavitation erosion was analyzed by scanning electron microscopy (JSM-840).

3 RESULTS AND DISCUSSION

3.1 Microstructure of weldment

The microstructure of weldment is inhomogeneous which falls into the weld zone (WZ), the heat-affected zone (HAZ) and the base metal in a simple way because of rapid heating to high temperature, rapid cooling and filler material during welding^[12]. Fig. 1(a) shows the three zones of the NAB weldment. The microstructure of the base metal is shown in Fig. 1(b), which comprises light etching area of α phase which is an FCC copper-rich solid solution, dark etching region of the lamellar eutectoid phases, and intermetallic κ phases of various morphologies. The dendritic particles of about 10 μm are κ_{II} , the particles less than 1 μm in α phase are κ_{IV} and the eutectoidal intermetallic phase which appears with a lamellar or globular morphology is κ_{III} ^[13, 14].

Because the HAZ was heated to about 950 – 1 000 °C^[6] during welding, the eutectoidal phase dissolved and transformed into β phase. During the

subsequent rapid cooling the high temperature β phase transformed to martensite. Therefore, the microstructure of HAZ consists of α phase, martensite and κ (κ_{II} , κ_{IV}) phase as shown in Fig. 1(c).

Because of rapid cooling, the microstructure of the WZ comprises very fine light etching α phase, martensite and small amount of κ (κ_{II}) phase in comparison with the base metal as shown in Fig. 1(d).

3.2 Mass loss

Fig. 2(a) shows the curves of the cumulative mass loss of the specimens of the WZ and the base metal versus cavitation erosion time. The cumulative mass loss of both zones increases with the erosion time. After 30 min of cavitation erosion the increment of the cumulative mass loss of the base metal becomes larger than that of the WZ, which means the base metal loses mass faster than the WZ does. After 2.5 h of cavitation erosion, the specimen of the base metal loses metal 17.5 mg while the WZ, only loses 12.1 mg. Fig. 2(b) shows the curves of the mass loss rate of the two areas against the erosion time. The mass loss rate goes up swiftly with time, but slows down after 2 h. The mass loss rate of the base metal is larger than that of the WZ. After 2.5 h of cavitation erosion, the mass loss rate of the base metal is 9.6 $\text{mg} \cdot \text{h}^{-1}$ while that of the WZ is 7.6 $\text{mg} \cdot \text{h}^{-1}$. These results indicate that the cavitation erosion resistance of the WZ is better than that of the base metal. Figs. 1(b) and 1(d) show that the grains of the WZ are much finer than that of the base metal. It is all known that the smaller the material grain size is, the better the mechanical properties are. The cavitation erosion resistance of a material is positive correlated with their mechanical properties^[11]. That's why the WZ possesses better resistance to cavitation erosion than the base metal does.

According to Preece^[15], the curve of the mass loss rate consists of four zones. The first of them is the incubation zone, in which there is no detectable mass loss. The second is the accumulation zone, in which the rate of mass loss increases to a maximum level. The third is the attenuation zone, in which the rate of mass loss decreases, and the fourth is the steady-state zone which depends on the characteristics of the material itself. In the present study on the NAB weldment, the incubation zone was not detected. The attenuation zone and the steady-state zone did not appear, which may be attributed to the short testing time.

3.3 Morphology of specimens after cavitation erosion test

Fig. 3 is the SEM micrographs of NAB weld

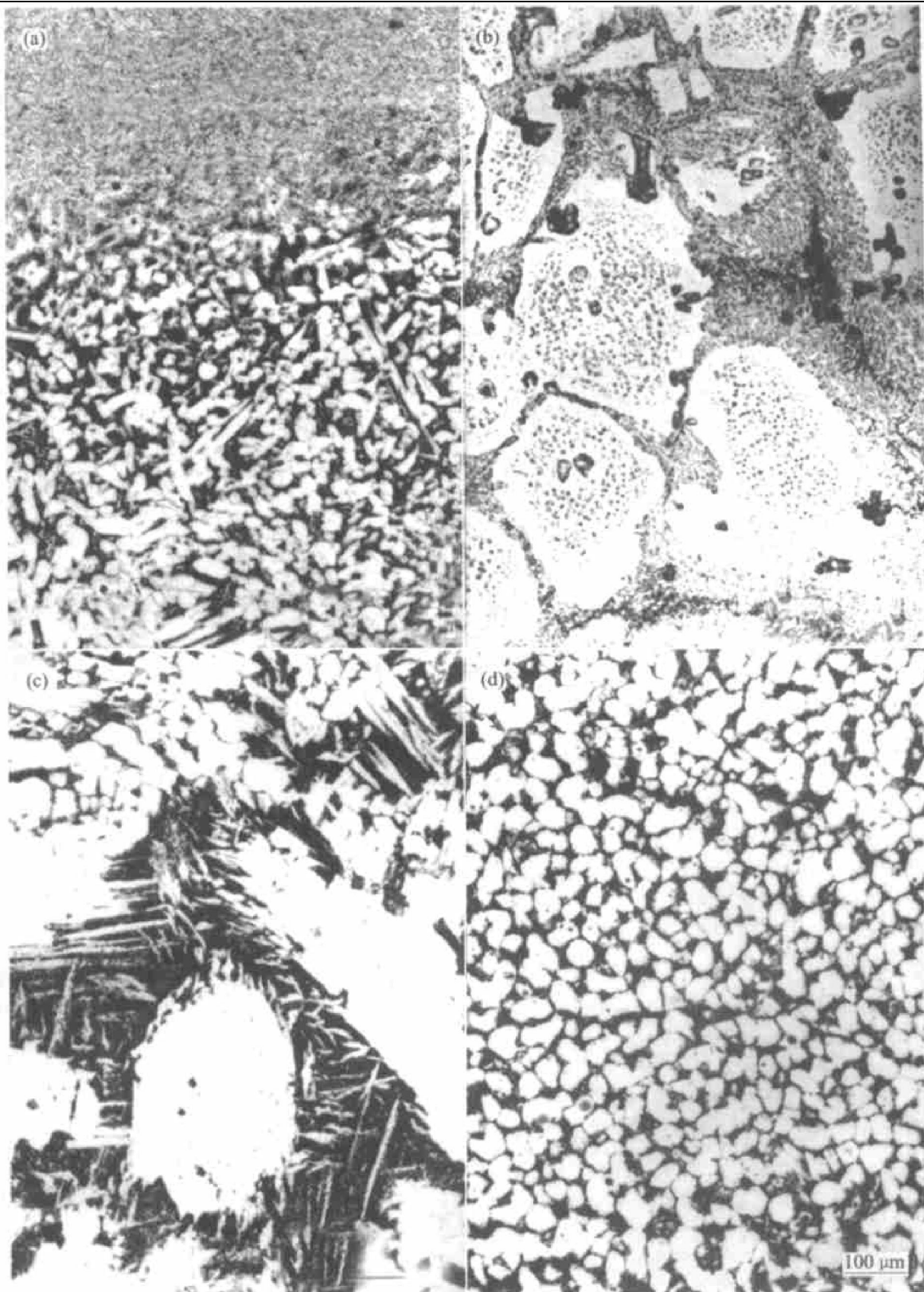


Fig. 1 Microstructures of NAB weldment(a), WZ(b), HAZ(c) and base metal(d)

ment after cavitation test for 10 min in 3.5% NaCl aqueous solution. It shows deformation of the specimen surface, formation of microvoids on the surface, slip lines in the α phases of the HAZ and the base metal and grooves along some of the boundaries of the α -martensite (in the HAZ) and the α -eutectoid phase

(in the base metal).

After 30 min of cavitation erosion, the α phase deformed severely and grooves and microvoids formed along phase boundaries in the WZ (Figs. 4(a) and 4(b)). In the HAZ, α phase continued to slip, microvoids formed and grew in the α phase

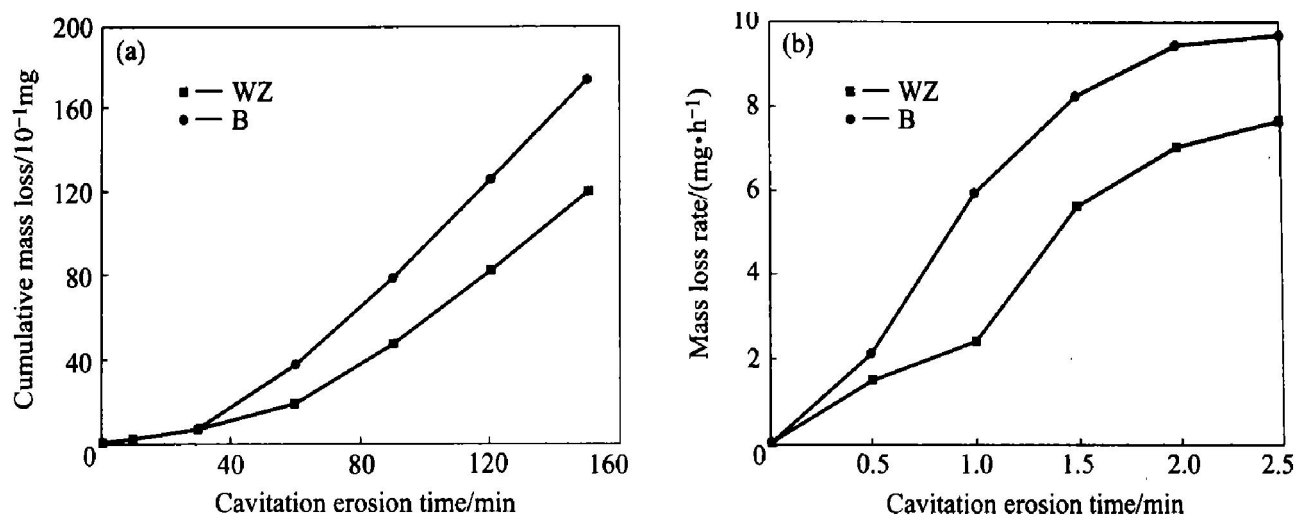


Fig. 2 Cumulative mass loss(a) and mass loss rate(b) as a function of cavitation erosion time of weld zone(WZ) and base metal(B) of NAB weldment



Fig. 3 SEM micrographs of NAB weldment after cavitation test in 3.5% NaCl aqueous solution for 10 min

(a) —Deformation of WZ; (b) —Microvoids and slip line in α phase of HAZ;
(c) —Microvoids and slip lines in α phase of base metal

and grooves formed along the phase boundaries while the martensite did not deform except some microvoids scattering in it (Figs. 4(c) and 4(d)). In the base metal, microvoids grew and merged, grooves along phase boundaries deepened, and the eutectoidal phase ($\alpha + \kappa_{\text{III}}$) and the edge of α phase suffered removal of mass (Figs. 4(e) and 4(f)).

One hour of cavitation erosion made the surface of the specimen rough. Traces of remained phases can still be seen (Fig. 5). In the WZ phase, boundaries were attacked more severely than α phases (Figs. 5(a) and 5(b)). In the HAZ some of the martensite still remained unattacked, though the α phase became very rough due to removal of mass (Figs. 5(c) and 5(d)). In the base metal not all of the α phases were damaged (Fig. 5(e)).

From Fig. 4 and Fig. 5 we can see that the phases of the NAB weldment are selected to attack. The martensite is preferential to be attacked in the WZ; the α phase, in the HAZ; and the eutectoidal phase ($\alpha + \kappa_{\text{III}}$), in the base metal.

After 2.5 h of testing the surface of specimens became even rougher. Traces of remained phases disappeared. Among the three zones the base metal was attacked most severely; the HAZ, less and the WZ,

the least (Fig. 6). Large cavities appeared on the surface in the base metal area (Figs. 6(e) and 6(f)).

3.4 Effect of NAB weldment microstructure on cavitation damage

Phase components and their crystal structures of a material have great effect on initiation and propagation of microcracks and removal of mass of the material during cavitation erosion. As mentioned above, the WZ of NAB weldment consists of α phase, martensite and small amount of κ phase; the HAZ, α phase, martensite and κ phases; and the base metal, α phase, eutectoidal phase ($\alpha + \kappa_{\text{III}}$) and various κ phases. The size of phases both in the HAZ and in the base metal is much larger than that in the WZ. Crystal structures of these phases are quite different. The α phase is FCC; the martensite, BCC; and the κ phase, CsCl type B2^[14]. And they differ from one another in response to the stress pulses created by collapse of bubbles during cavitation. The α phase is the initial phase to slip and deform. In the WZ, deformation of α phase is hindered by phase boundaries, which causes stress concentration there. Microvoids form in the local areas there (Fig. 3(a)). As cavitation erosion going on, the microvoids grow

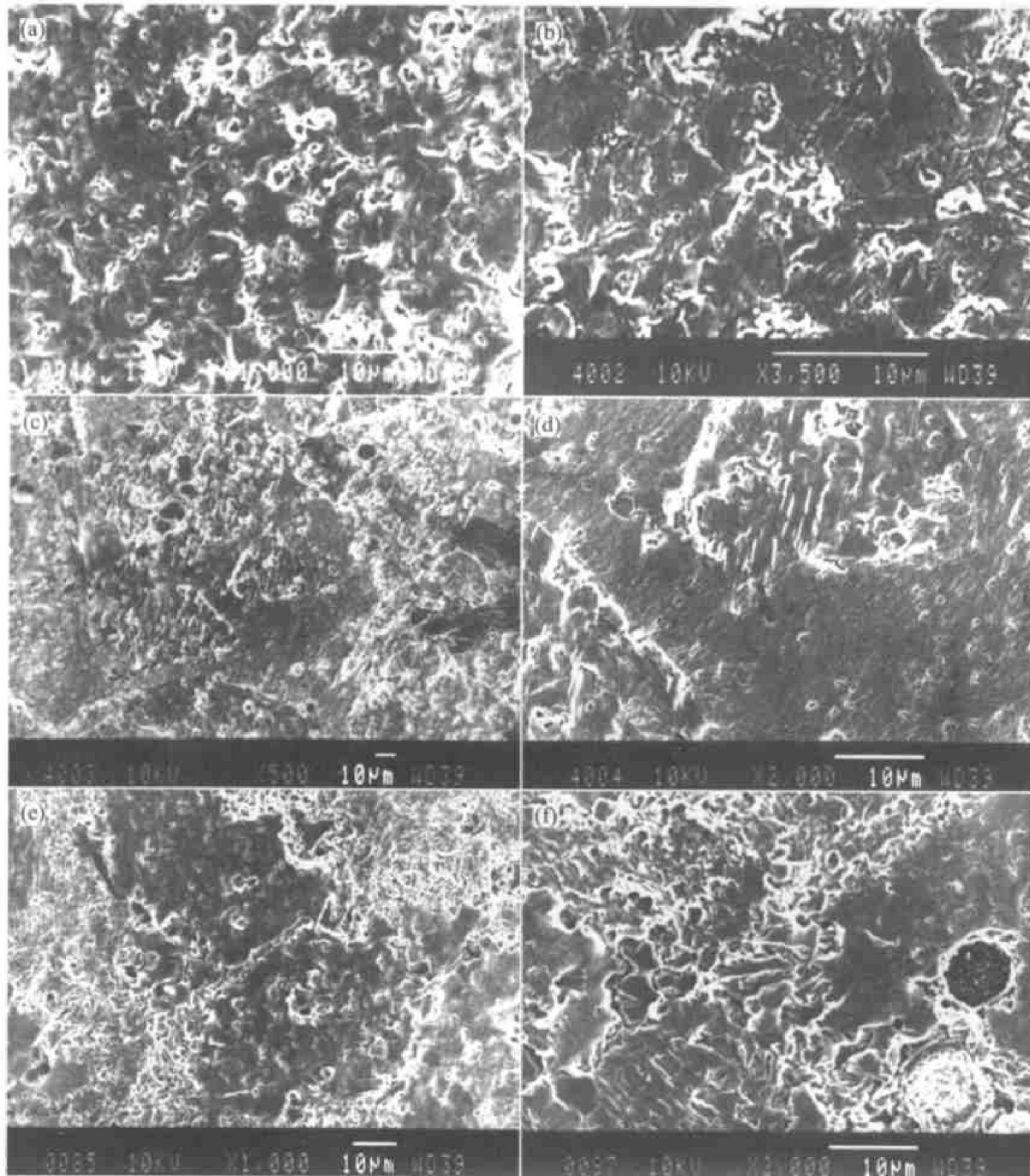


Fig. 4 SEM micrographs of NAB weldment after cavitation test in 3.5% NaCl aqueous solution for 30 min

- (a), (b) —Severe deformation of α phase, formation of grooves and microvoids along phase boundaries in WZ;
 (c), (d) —Slip steps and microvoids in α phase and grooves along phase boundaries in HAZ;
 (e), (f) —Metal loss of eutectoidal phase, grooves along phase boundaries and voids in α phase and eutectoidal phase in base metal

and link, and then microcracks form (Figs. 4(a) and 4(b)). The cracks propagate in the α phase, which results in removal of α phase in the end (Figs. 5(a) and 5(c)). In the HAZ, deformation of the α phase is hindered by the martensite around it and κ phases inside it. Slip steps pile up mainly in the edge areas of α phase (Fig. 3(b)). Microvoids form here, and then grow and link into microcracks. Microvoids also form in other area of the α phase (Fig. 7). The microcracks propagate into the α phase and link to the growing microvoids, which results in removal of part of the α

phase (Figs. 4(c) and 4(d)). The microcracks propagate into depth of α phase and into martensite, which causes damage of α phase and martensite (Figs. 5(c) and (d)). In the base metal, deformation of α phase is similar to that in the HAZ. And the slip steps also pile up mainly in the edge area of α phase (Fig. 3(c)). Microcracks initiate in the edge area of α phase and around κ phases. The lamellar κ_{III} phase of eutectoid phase ($\alpha + \kappa_{III}$) possesses low damage resistance and is easy to break and to be

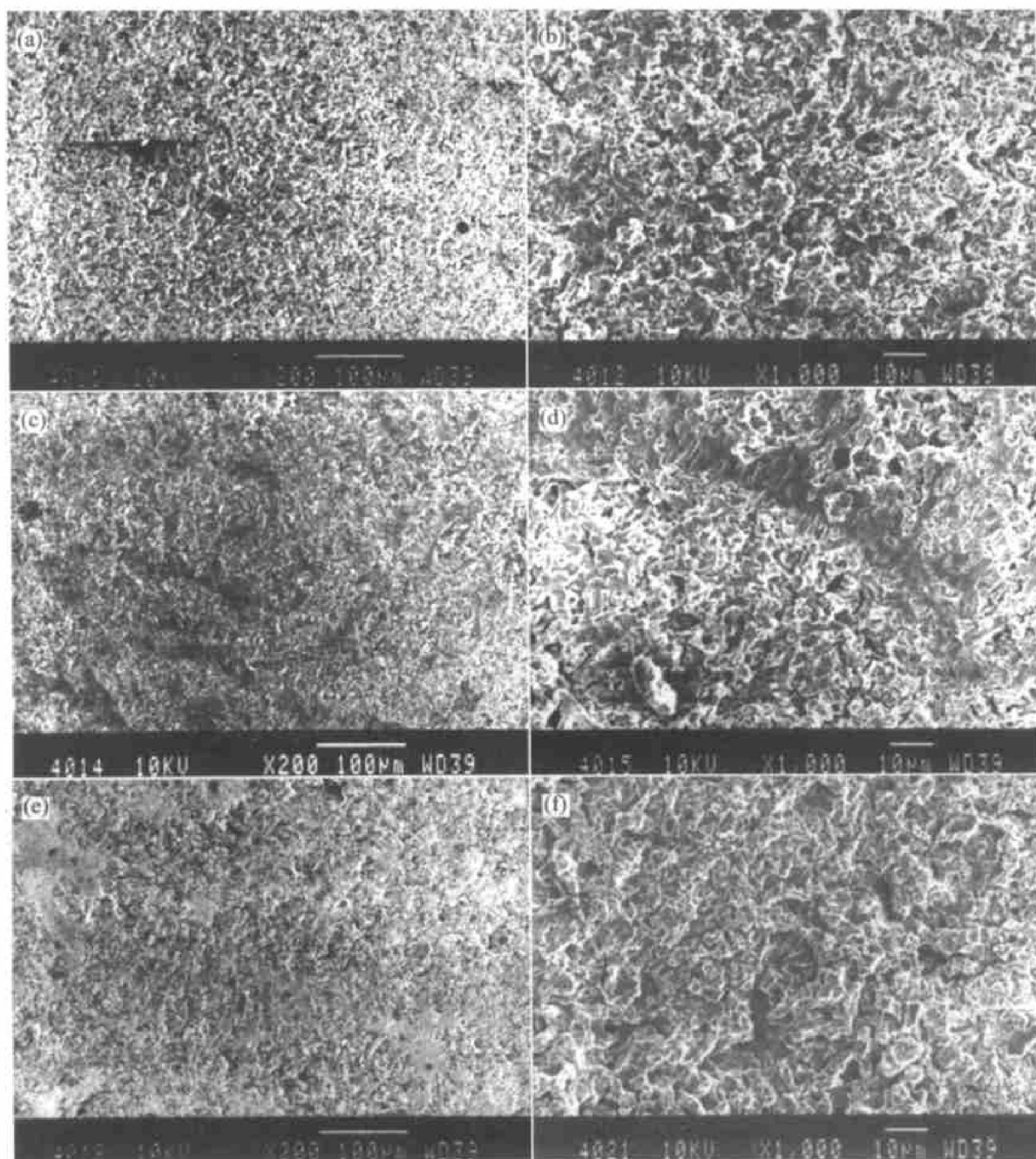


Fig. 5 SEM micrographs of Ni-Al bronze weldment after cavitation test in 3.5% NaCl aqueous solution for 1 h
 (a), (b) —Rough surface of WZ; (c), (d) —Remain of martensite fragments in HAZ;
 (e) and (f) —Rough surface of base metal

removed under stress of cavitation erosion. Therefore, the eutectoidal phase ($\alpha + \kappa_{III}$) is badly damaged after cavitation eroded for 30 min (Figs. 4(e) and (f)). As cavitation erosion going on, microcracks propagate into depth of the eutectoidal phase ($\alpha + \kappa_{III}$) and κ phases and into the α phase, which results in formation of cavities, removal of κ_{II} phase and damage of α phase (Figs. 5(e), 5(f), 6(e) and 6(f)).

4 CONCLUSIONS

1) The WZ possesses better cavitation erosion

resistance than the base metal does. After cavitation eroded for 2.5 h the cumulative mass loss of the WZ is about 2/3 of that for the base metal; and the mass loss rate of the WZ is some 3/4 of that for the base metal.

2) At the early stage of cavitation erosion, the phases of the weldment microstructure undergoing selective attack by the stress of cavitation erosion are: martensite in the WZ, α phase in the HAZ and eutectoidal phase in the base metal.

3) The microcracks initiate at the phase boundaries, then propagate into the easily damaged phases,

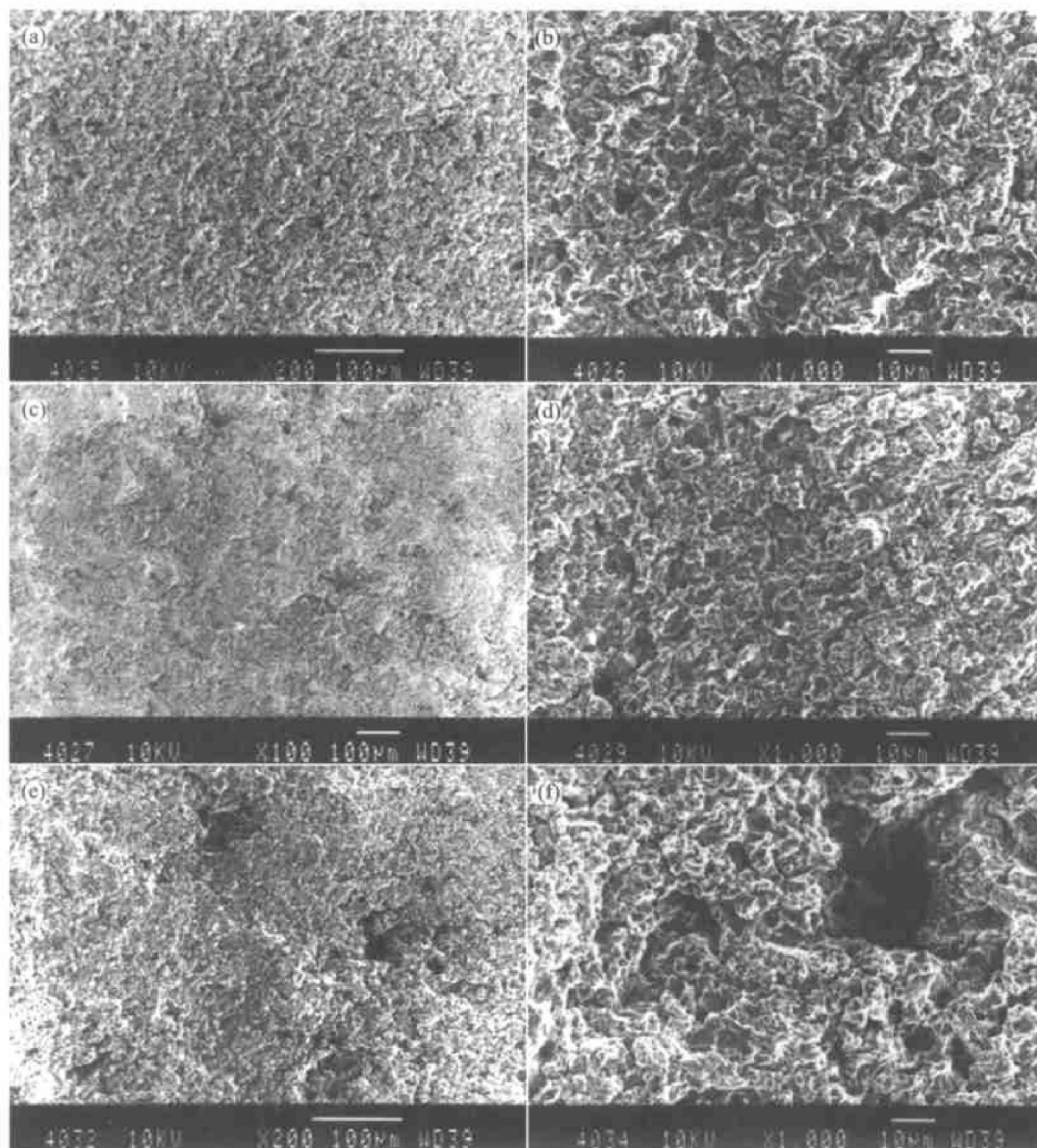


Fig. 6 SEM micrographs of NAB weldment after cavitation test in 3.5% NaCl aqueous solution for 2.5 h
(a), (b) —Damage surface of WZ; (c), (d) —Damage surface of HAZ;
(e), (f) —Cavities on damaged surface of base metal

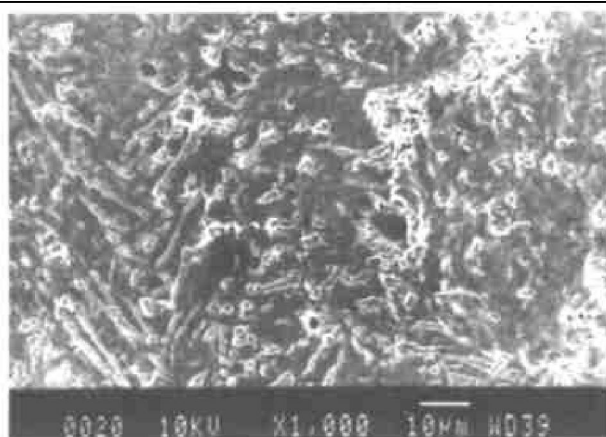


Fig. 7 SEM micrographs of NAB weldment after cavitation test in 3.5% NaCl aqueous solution for 0.5 h
(microvoids along phase boundaries and in α phase)

and result in the damage of the whole surface of specimen in the end.

ACKNOWLEDGEMENT

The authors would like to thank Prof. WEI Xi-ang-yun, YAO Zhi-ming and ZHENG Yu-gui of Shenyang Metal Research Institute, Chinese Academy of Science (CAS) for their help.

REFERENCES

- [1] Karimi A, Martin J L. Cavitation erosion of materials [J]. Int Met Rev, 1986, 31(1): 1-26.
- [2] Budiski K G. Surface Engineering for Wear Resistance [M]. New York: Prentice Hall, 1988. 24-26.
- [3] Clews K J. Evaluated temperature properties of aluminum

- bronze(alloy D) parent metal rod and weld metal[J]. British Welding Journal, 1966, 13(8): 476 - 483.
- [4] Clews K J. Metallurgical aspect of aluminum bronze welding problems[J]. British Welding Journal, 1965, 12(3): 126 - 144.
- [5] Foster M L, Goldspiel S. Weldable as-cast nickel aluminum bronze—composition and microstructure[J]. AFS Trans, 1961, 69: 80 - 100.
- [6] Sahoo M. Weldability of nickel-aluminum bronze alloy C95800[J]. AFS Trans, 1982, 90: 893 - 911.
- [7] Sadayappan M, Letts M W, Sahoo M. Simulation of weld cracking in heat affected zone of aluminum bronze alloy C95800[J]. AFS Trans, 2000, 108: 725 - 732.
- [8] Zanis C A, Ferrara R J. An investigation into dealloying of cast Ni-Al bronze[J]. AFS Trans, 1972, 80: 259 - 267.
- [9] Zanis C A, Ferrara R J. Sea water corrosion of nickel-aluminum bronze[J]. AFS Trans, 1974, 82: 71 - 78.
- [10] Lorimer G W, Hasan F, Iqbal J, et al. Observation of microstructure and corrosion behavior of some aluminum bronzes[J]. British Corrosion J, 1986, 21(4): 244 - 248.
- [11] ASTM Standard G32-92. Standard Test Method for Cavitation Erosion using Vibratory Apparatus, in: Annual Book of ASTM Standard, Vol. 03. 02, ASTM, Philadelphia
- [12] ZHANG W Y. Metallurgy of Welding[M]. Beijing: China Machine Press, 1997. 188 - 189. (in Chinese)
- [13] Hasan F, Jahanafrooz A, Lorimer G W, et al. Morphology, crystallography, and chemistry of phases in as-cast nickel-aluminum bronze[J]. Metall Mater Trans, 1982, 13A: 1337 - 1345.
- [14] Brezina P. Heat treatment of complex aluminum bronze [J]. Inter Met Rev, 1982, 27(2): 77 - 120.
- [15] Preece C M. Cavitation erosion[A]. Treatise on Material Science and Technology [C]. C M Preece, New York, NY: Academic Press, 1979. 249 - 268.

(Edited by HUANG Jin-song)